Int. J. Rock Mech. Min. Sci. & Geomech. Abstr. Vol. 30, No. 2, pp. 71–79, 1993
Printed in Great Britain. All rights reserved

0148-9062/93 $6.00 + 0.00
Copyright © 1993 Pergamon Press Ltd

Evaluation of Groundwater Flow into Mined Panels

Z. OUYANG†
D. ELSWORTH‡

The impact of underground mining on groundwater flow around a mined panel is quantified. A model is structured to represent strata deformation and concurrent steady fluid flow in a naturally fractured medium as a result of underground mining. The model conceptually represents mechanisms of hydraulic conductivity enhancement caused by deformation through use of a modulus reduction ratio R_m. The modulus reduction ratio R_m is incorporated in the expression for hydraulic conductivity to account for the influence of joint aperture and spacing, joint stiffness and modulus of the intact rock, on changes in hydraulic conductivity. The resulting relations for hydraulic conductivity avoid the requirement of independently determining joint stiffness, as apparent in previous formulations. Panel inflows are defined for a variety of possible geometric and mechanical configurations. Flux charts are developed for straightforward practical use. The resulting charts are verified using two case studies. These reveal that changes in strata conductivities are strongly related to deformations induced by underground mining. Excellent agreement has been achieved.

INTRODUCTION

Determination of the dewatering behavior above high extraction ratio coal mining (longwall mining) has been the highlight of considerable research [1]. The disruption of groundwater supplies in the vicinity of underground coal mining occurs often as a result of failure of the overlying strata. The severity of failure, resulting from mining induced displacement fields in the overburden, controls the degree of modification in the groundwater regime. Formation of an underground void emplaces a hydraulic sink within the strata to which groundwater may preferentially flow. According to the mixed responses of groundwater regimes recorded as a result of longwall mining [1], depressed ground water levels may never stabilize, may stabilize at depressed levels, or may rebound, approaching premining levels, when mining is completed. In particular, when the local aquifers are being used for domestic or industrial water supplies, these impacts are of significant concern.

Hydraulic conductivity around a working panel is modified by mining activities. Where groundwater moves nearly exclusively through an equivalent porous medium of interconnected fractures, the system may be represented as an equivalent network. Mining-induced fracturing and dilation of joints and bedding planes increases the hydraulic conductivity and porosity of the strata, enhances hydraulic connections between aquifers and the mine, and alters the groundwater hydrology of aquifers. Longwall mining results in rapidly completed subsidence over the panel, major strata movement and fracturing throughout the overburden, and rapid aquifer response. To simulate fluid flow in such a medium, complex behavior, involving coupled fluid flow and solid deformation, should be represented. This is completed in this work.

Various studies [2–5] have demonstrated the considerable hydrologic effect of subsidence on the overlying aquifers. Potentiometric levels decline, as a result of increased losses from aquifers and also due to increased hydraulic conductivity within aquifers (changing local hydraulic gradients) and increase in fracture-storativity (creating temporary head drops).

Dimensional analysis is used in this work to define total groundwater inflow into mined excavations. A conceptual model is developed, assuming that the fractured rock mass behaves as an equivalent porous medium with fractures dominating the flow pattern. Hydraulic conductivity is enhanced by deformation induced through mining. Bulk strains are partitioned between the fractures and the intact rock material and define the magnitude of conductivity enhancement. The strain partitioning is controlled by a modulus reduction ratio R_m that may be correlated with existing rock mass classification systems.

†Department of Mining Engineering, Wuhan Iron and Steel University, Wuhan, Hubei, Peoples' Republic of China; currently at Department of Mineral Engineering, Pennsylvania State University.
‡Department of Mineral Engineering, Mineral Sciences Building, Pennsylvania State University, University Park, PA 16802, U.S.A.

PARAMETER DETERMINATION FOR ROCK MASSES

In the coal measure rocks of interest here, fracture conductivities are commonly orders of magnitude larger than the porous medium. Correspondingly, mass conductivity may be adequately represented by an equivalent fracture network, where fractures obey the cubic law. This representation is convenient since it enables changes in conductivity that result from body strains to be straightforwardly evaluated.

Hydraulic conductivity enhancement

The hydraulic conductivity [6] K of a set of parallel fractures of spacing S and aperture B may be defined as:

$$K = \frac{gB^3}{12\mu_k S}, \tag{1}$$

where g is gravitational acceleration and μ_k is kinematic viscosity. Equation (1) expresses the conductivity in the absence of deformation ($\Delta\epsilon_x = \Delta\epsilon_y = 0$) and for a prescribed initial fracture aperture. Assume that the normal displacement over a fracture, induced by stress change, is Δu_j. By inspection of equation (1), it is convenient to incorporate Δu_j into the expression of hydraulic conductivity K as:

$$K_x = \frac{g}{12\mu_k S}(B + \Delta u_{jy})^3 \tag{2}$$

and

$$K_y = \frac{g}{12\mu_k S}(B + \Delta u_{jx})^3, \tag{3}$$

where Δu_{jx} and Δu_{jy} are, respectively, the displacements in the x- and y-directions, on fractures that are orthogonal to the displacement.

Defining the normal strain across a fracture, induced by stress change, as $\Delta\epsilon$ and assuming that individual fractures are distinctly soft with respect to the porous medium, then deformation modified hydraulic conductivity K may be written as [7]:

$$K = \frac{g}{12\mu_k S}(B + S\,\Delta\epsilon)^3, \tag{4}$$

where appropriate strain components are utilized. With the further assumption that the spacing of the fracture S is much greater than the aperture of the fracture B, the modified hydraulic conductivity of a single fracture set that incorporates solid deformation, may be calculated using:

$$K = \frac{g}{12\mu_k S}\left(B + \frac{ES\,\Delta\epsilon}{k_n S + E}\right)^3 \tag{5}$$

where k_n is the normal stiffness of the fractures. E is the modulus of the rock matrix and $\Delta\epsilon$ is the strain in the direction perpendicular to the fractures. Although equation (5) is straightforward and the parameters for spacing S and initial aperture B may be readily determined from field tests, magnitudes of fracture stiffness k_n remain elusive. Empirical data for k_n are meager. An indirect method for predicting the stiffness of fractures k_n is developed in the following.

Modulus reduction ratio R_m

Modulus reduction ratio R_m may be defined as:

$$R_m = \frac{E_m}{E}, \tag{6}$$

where E_m and E are, respectively, the rock mass modulus and rock matrix modulus under uniaxial compressive loading.

Walsh and Brace [8] derived approximate mathematical expressions for the modulus reduction ratio of a material which contains a dilute concentration of spherical cavities and elliptical cracks. The expressions of R_m have been available for the two conditions where "all cracks are open" and secondly where "all cracks are closed". Hobbs [9] further proposed that asperities on rock fractures (assumed normal to the direction of uniaxial loading) may be represented as minature circular loading areas through which stress is transmitted. The resulting variations of modulus reduction ratios R_m with defect concentration exhibit a similar pattern to *in situ* test data [9].

From Hooke's law, for a linear rock matrix:

$$\Delta\epsilon_s = \frac{\Delta\sigma}{E}, \tag{7}$$

where $\Delta\epsilon_s$ is the strain in the direction of the applied stress $\Delta\sigma$, and E is the modulus of deformability of the rock matrix. Therefore, displacement in a segment of the rock matrix bounded between two fractures at separation S, is $\Delta u_s = \Delta\epsilon_s S$.

Under the same applied stress $\Delta\sigma$, the deformation across a single fracture Δu_j is:

$$\Delta u_j = \frac{\Delta\sigma}{k_n}, \tag{8}$$

where k_n is the normal fracture stiffness. Total displacement Δu is obtained from the sum of component displacements, as:

$$\Delta u = \Delta u_j + \Delta u_s, \tag{9}$$

enabling the average strain $\Delta\epsilon$ to be defined from combining equations (7) and (8) as:

$$\Delta\epsilon = \frac{\Delta u_j + \Delta u_s}{S + B} = \left[\frac{S}{E(S+B)} + \frac{1}{k_n(S+B)}\right]\Delta\sigma. \tag{10}$$

From equation (10), the modulus of the rock mass may be extracted as:

$$E_m = \frac{(S+B)Ek_n}{Sk_n + E}, \tag{11}$$

or rearranging through substitution into equation (6) as:

$$R_m = \frac{E_m}{E} = \frac{1 + \dfrac{B}{S}}{1 + \dfrac{E}{Sk_n}}. \tag{12}$$

The resulting modulus reduction ratio R_m is a function of fracture porosity B/S and mass compliance ES/k_n. Theoretically, R_m varies between zero [$E/(Sk_n) \gg B/S$] and unity [$E/(Sk_n) = B/S$].

If the ratio E/k_n is known for a given rock mass, the modulus of the rock mass may be determined directly. Unfortunately, the ratio E/k_n has wide variability. It varies with experimental procedure and rock types. The ratio has been determined of the order as 0.1/cm (0.04/in.) in some experiments [10, 11] on basalts, granite and marble. Peres-Rodrigues [12] determined ratios of: 0.08485/m for limestone, 0.15116/m for gneiss and 0.04168/m for granite.

Alternatively, R_m may be determined for a particular rock mass from various rock mass classifications and used to define the ratio E/Sk_n. This latter mode is preferred. Rearranging equation (11) for k_n returns:

$$k_n = \frac{E_m E}{E(S+B) - E_m S}. \tag{13}$$

If it is possible to estimate the parameters on the right-hand side of equation (13), then fracture stiffness k_n may be determined indirectly. Alternatively, if the modulus reduction ratio R_m is known, k_n may be expressed, by rearranging equation (12) as:

$$k_n = \frac{R_m E}{S\left(1 - R_m + \dfrac{B}{S}\right)}. \tag{14}$$

It is in this form that normal stiffness is most conveniently and usefully defined in determining the partitioning of body strains between matrix and fracture as required by equations (2) and (3).

Fracture normal displacement Δu_j

Hydraulic conductivity can be expressed as a function of fracture aperture B and normal displacement Δu_j. Around a mined panel, the spatial distribution of induced total displacements Δu may be calculated. The ratio R_m controls the partitioning of the total displacements between the matrix and fracture systems.

The total displacement Δu in equation (9) can be represented by the matrix and fracture components as:

$$\Delta u = S\,\Delta\epsilon_s + \Delta u_j, \tag{15}$$

where $\Delta\epsilon_s$ is the strain in the rock matrix. As a result of stress equilibrium:

$$\Delta\sigma_s = \Delta\sigma_j, \tag{16}$$

where $\Delta\sigma_s$ and $\Delta\sigma_j$ are, respectively, the stresses in the rock matrix and fracture. In terms of displacements, equation (16) can be written as:

$$\frac{\Delta u_s E}{S} = \Delta u_j k_n, \tag{17}$$

where Δu_s and Δu_j are, respectively, displacements within the rock matrix and the fracture, and $\Delta\epsilon_s = \Delta u_s/S$. From equations (15) and (17), the ratio is obtained:

$$\frac{\Delta u_j}{\Delta u} = \frac{\Delta u_j}{S\,\Delta\epsilon_s + \Delta u_j} = \frac{\Delta u_j}{\dfrac{S\,\Delta u_j k_n}{E} + \Delta u_j} = \frac{E}{Sk_n + E}. \tag{18}$$

Furthermore, rearranging equation (18) returns:

$$\Delta u_j = \frac{E\,\Delta u}{Sk_n + E} = \frac{E(S+B)\Delta\epsilon}{Sk_n + E}, \tag{19}$$

where displacement is controlled by elastic parameters E and k_n and geometric parameters of spacing and fracture aperture.

Substituting equation (14) into equation (19) yields:

$$\Delta u_j = [(1 - R_m)S + B]\,\Delta\epsilon. \tag{20}$$

Incorporating equation (20) into the relations describing hydraulic conductivity of equations (2) and (3) returns:

$$K_x = \frac{g}{12\mu_k S}\{B + [S(1 - R_m) + B]\Delta\epsilon_y\}^3 \tag{21}$$

and

$$K_y = \frac{g}{12\mu_k S}\{B + [S(1 - R_m) + B]\Delta\epsilon_x\}^3. \tag{22}$$

Behavior is bounded by the two extreme instances where $R_m = 0$ and $R_m = 1$. Assuming first $R_m = 0$, then the modulus E_m of the rock mass is zero and vertical hydraulic conductivity K_y becomes:

$$K_y = \frac{g}{12\mu_k S}[B + (S+B)\Delta\epsilon_x]^3. \tag{23}$$

This implies that the fractures are so soft that all the deformation in the rock mass is concentrated on the fractures. As a consequence, the change in hydraulic conductivity K_y is a maximum. Alternatively, when $R_m = 1$, the modulus of the rock mass is equivalent to the intact modulus E of the rock. Equation (22) then becomes:

$$K_y = \frac{g}{12\mu_k S}[B + B\,\Delta\epsilon_x]^3, \tag{24}$$

reflecting the behavior anticipated for the homogeneous case.

Geomechanics Classification

As is apparent from the preceding, changes in hydraulic conductivity may be directly indexed to the modulus reduction ratio R_m. This is particularly useful since modulus reduction ratios may be determined directly from a variety of rock mass classification systems. One such system is the Geomechanics Classification, or the Rock Mass Rating (RMR) system, as developed by Bieniawski [13]. This engineering classification for rock masses utilizes six parameters, all of which are measurable in the field. The Geomechanics Classification has been used extensively in mining [14, 15], particularly in the U.S., and has also been applied to rock foundations [16] and slopes [17]. In the case of rock foundations, the Rock Mass Rating (RMR) from the Geomechanics Classification has been related to the *in situ* modulus of deformation [18, 19].

Since the deformability modulus of a rock mass depends directly on fracture frequency I (or fracture spacing S), fracture spacing may be used in determining R_m from the RMR system. Similar to other parameters

Table 1. Classification of parameters of rock masses

	Ranges of values				
S_c(m)	> 2	0.6–2	0.2–0.6	0.06–0.20	< 0.06
S(m)	2	1	0.5	0.2	0.05
B(m)	10^{-5}	10^{-4}	10^{-3}	2×10^{-3}	5×10^{-3}
R_m	1	0.8	0.6	0.4	0.2
R_{m1}	1–0.93	0.93–0.80	0.0–0.57	0.57–0.20	0.28–0.0
R_{m2}	1–0.96	0.96–0.87	0.87–0.7	0.70–0.40	0.40–0.00

S_c = values from [13].
R_{m1} = gneiss [12].
R_{m2} = limestone [12].

in the RMR system, fracture spacings are divided into five groups to represent a spectrum of rock mass types. Taking an average value for each of the groups, as $S = (>)$ 2.0, 1.0, 0.5, 0.2, $(<)$ 0.05 (m) and $B = 10^{-5}$, 10^{-4}, 10^{-3}, 2×10^{-3}, 5×10^{-3} (m) and assuming that the modulus reduction ratio is "linearly" distributed within the five groups yields representative values of $R_m = 1.0$, 0.8, 0.6, 0.4, 0.2. The values are summarized in Table 1 which can be verified from the experimental results of other researchers [8, 9, 12].

FINITE ELEMENT MODELING

Changes in hydraulic conductivity may be determined directly from known or prescribed induced displacements. The distribution of induced displacements may also be determined. In this work, a finite element model is developed to calculate displacements around and, total fluxes into, the excavation. The FE model incorporates hydraulic conductivity enhancement in deforming strata containing natural fractures. Deformations throughout the elastic body induce changes in aperture of individual fractures that may drastically change hydraulic conductivity distributions.

The following development is restricted to 2-D elasticity with concurrent fluid flow. Governing equations are developed to represent the development of the deformation and flux fields resulting from applied boundary conditions. The equations are subsequently cast in finite element format and coupled to represent the steady-state response due to mining.

In the most general form, stress–strain relations for the solid phase can be expressed as:

$$\Delta\sigma = \mathbf{D}\,\Delta\epsilon, \tag{25}$$

where $\sigma = (\sigma_x, \sigma_y, \tau_{xy})^T$ is the vector of stress components, ϵ represents corresponding strain components and $\mathbf{D}$ is a matrix of elastic coefficients. Applying the principle of virtual work and ignoring body forces, nodal displacements $\hat{\mathbf{u}}$ are related to nodal forces $\mathbf{F}$ as:

$$\mathbf{G}_s\hat{\mathbf{u}} = \mathbf{F}, \tag{26}$$

where $\mathbf{G}_s$ and $\mathbf{F}$ are respectively,

$$\mathbf{G}_s = \int_V \mathbf{B}^T\mathbf{D}\mathbf{B}\,dV \tag{27}$$

and

$$\mathbf{F} = \int_\Gamma \mathbf{N}^T\mathbf{T}\,d\Gamma, \tag{28}$$

where V is the volume of interest, Γ is the surface of the volume, $\mathbf{N}$ is a vector of shape functions, $\mathbf{b}$ is a matrix of shape function derivatives and $\mathbf{T}$ is a vector of surface tractions.

Assuming steady-state conditions for flow within the fluid phase, combination of the continuity relation and Darcy's law returns:

$$\nabla(\mathbf{K}\,\nabla h) = 0, \tag{29}$$

where $\nabla = (\partial/\partial x, \partial/\partial y, \partial/\partial z)$. Equation (31) may be written in finite element format by using the Galerkin method where $\mathbf{h}$ is a vector of nodal heads, h, $\mathbf{G}_f$ is a conductance

$$\mathbf{G}_f\mathbf{h} = \mathbf{Q} \tag{30}$$

matrix and $\mathbf{Q}$ is a vector of prescribed boundary fluxes.

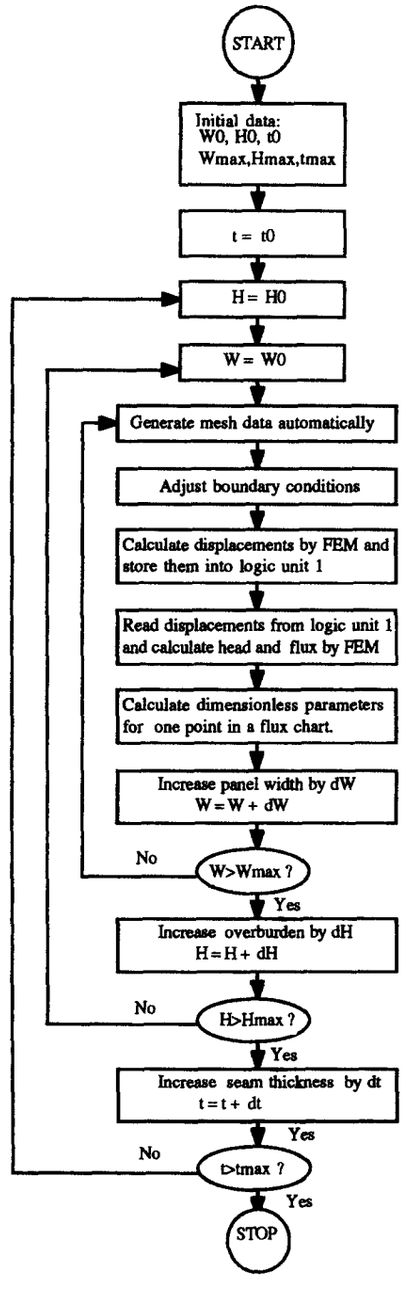

Fig. 1. Flowchart of FE model.

The conductivity matrix **G** is given as:

$$\mathbf{G}_f = \int_v (\nabla \mathbf{N}) \cdot \mathbf{K} \cdot (\nabla \mathbf{N})\, dV \tag{31}$$

and nodal fluxes are

$$\mathbf{Q} = \int_\Gamma \mathbf{N}\mathbf{n} \cdot \mathbf{K} \cdot (\nabla h)\, d\Gamma, \tag{32}$$

where Γ is the boundary segment.

In evaluating fluxes into the excavation, displacements induced by the mining process are first determined from the elastic model. Deformations are then incorporated into the hydraulic model to determine total inflows. An automeshing program is used in handling the onerous task of data preparation in the evaluation of flux charts through equations (26) and (30). This procedure is described in the flowchart of Fig. 1. Fluxes may be determined for a variety of mine panel geometric configurations and material parameters. To aid presentation of the resulting data, a minimum set of dimensionless groupings are determined from the full set of system parameters.

DIMENSIONLESS PARAMETERS

The basic variables of geometry and material properties that describe the behavior of the coupled flow–deformation system may be rearranged into a minimum set of dimensionless groupings. This exercise is most usefully completed if the flow and deformation system are considered individually. Changes in flow result from changes in hydraulic conductivity that in turn result from the induced deformation field. Choosing this hierarchy, that deformation controls flow through the distribution of body strains, it is appropriate to first consider the controls on deformation.

Parameters defining body displacements

The distribution of body strain $\Delta\epsilon$ is controlled by the geometric and material parameters described in Fig. 2, namely, width of the panel W, depth of the seam H, seam thickness t, rock mass modulus E_m, unit weight of the rock γ and Poisson's ratio v. Correspondingly, the minimum set of dimensionless parameters may be defined as:

$$\Delta\epsilon = f\left[\frac{W}{H};\ \frac{t}{H};\ \frac{E_m}{\gamma H};\ v\right], \tag{33}$$

where Poisson's ratio is of nominal influence and can be assumed to be of constant magnitude, $v = 0.25$, for all practical purposes. Therefore, strain distribution is controlled by both geometry and the dimensionless mass modulus of the surrounding material, through $E_m/(\gamma H)$. If force boundary conditions are applied to the excavation, then both geometric parameters, W/H and t/H are significant. If, however, complete closure of the opening is anticipated, as is the case in longwall mining, then the strain distribution is sensibly controlled only by the ratio of these parameters, or W/t. This corresponds to applied displacement boundary conditions and results in only a weak dependence on $E_m/\gamma H$. Consequently, in this work, the strain field is assumed to be defined by:

$$\Delta\epsilon = f\left[\frac{W}{t};\ \frac{E_m}{\gamma H};\ v = 0.25\right], \tag{34}$$

enabling changes in hydraulic conductivity distributions to be directly evaluated.

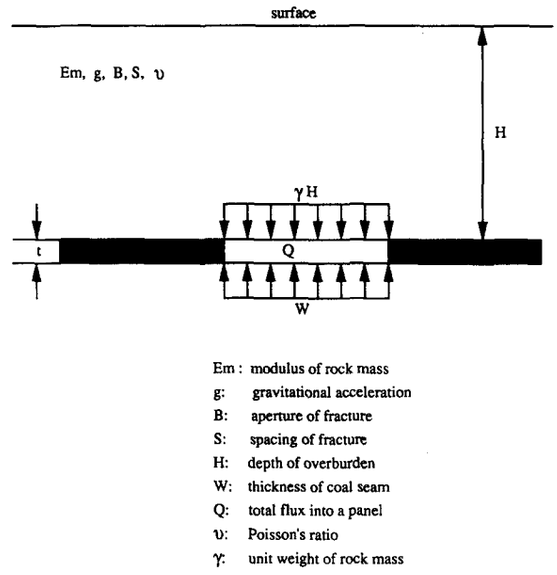

Fig. 2. Variables describing mine panel geometry.

Parameters defining flowrates

For flow into a panel set within a homogeneous medium, with the groundwater table at ground surface, then discharge rate per unit length Q may be defined in terms of the dimensionless groupings:

$$Q = f\left[\frac{W}{H};\ \frac{t}{H};\ K\right], \tag{35}$$

where K is the hydraulic conductivity, assumed invariant with strain in the first instance. For the slender panels of interest here, flowrate Q is insignificantly modified by the ratio t/H, enabling the nondimensional flowrate to be defined as:

$$\frac{Q}{KH} = f\left[\frac{W}{H};\ \Delta\epsilon\right], \tag{36}$$

where the influence of mining induced displacements is now inferred through the induced body strain field $\Delta\epsilon$. The significant parameters of interest, that relate to flow within a deforming fractured medium may be determined on using the definition of rock mass conductivity of equation (21) and (22), that may be rearranged to give:

$$\frac{Q}{KH} = \frac{12 Q \mu_k}{gHB^2}\left(\frac{S}{B}\right)\left\{1 + \left[\frac{S}{B}(1 - R_m) + 1\right]\Delta\epsilon\right\}^{-3}. \tag{37}$$

This further suggests that groundwater inflows may be defined in terms of the functional relation:

$$\frac{Q\mu_k}{gHB^2} = f\left[\frac{B}{S};\ R_m;\ \frac{W}{t};\ \frac{E_m}{\gamma H};\ v = \text{constant}\right], \tag{38}$$

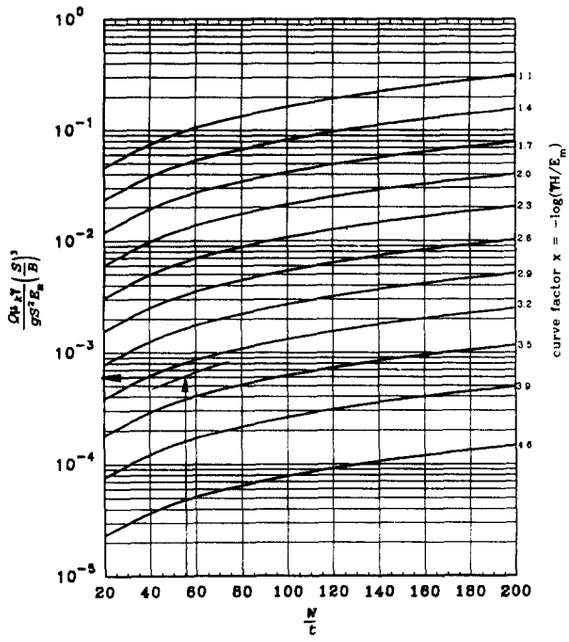

Fig. 3. Flux chart.

that may be further rearranged to yield:

$$\frac{Q\mu_k\gamma}{gS^2E_m}\left(\frac{S}{B}\right)^3 = f\left[\frac{B}{S};\ R_m;\ \frac{W}{t};\ \frac{E_m}{\gamma H};\ \nu = \text{constant}\right]. \tag{39}$$

In this manner, a different functional relation between dimensionless discharge Q_D dimensionless panel width W/t and dimensionless modulus $E_m/(\gamma H)$ may be defined for individual values of fracture porosity B/S and modulus reduction ratio R_m. To reduce the number of figures required in this form, the ratio B/S is linked directly to the modulus reduction ratio R_m as defined in Table 1.

Where values of both B and S are individually prescribed for individual magnitudes of R_m, one figure can represent the anticipated flow response, defined through the parameters W/t and $E_m/(\gamma H)$. If only the ratio B/S is linked uniquely with R_m, then a single figure is required to represent each fracture aperture magnitude B. The former approach is used in this study, as defined in Table 1.

Flux charts

Figure 3 shows a single chart based on this approach. The figure may be used through application of the following steps:

1. *In situ* hydraulic conductivity tests are completed to determine the pre-mining magnitudes of conductivity K and fracture spacing S. The equivalent fracture aperture B may be determined from equation (1).
2. With the ratio B/S defined, the modulus reduction ratio R_m is automatically defined from Table 1. Rock mass modulus E_m may be evaluated from equation (12) as $E_m = R_m E$, where E is the intact modulus of rock.
3. The parameters $E_m/(\gamma H)$ may be evaluated and the known geometry W/t used to determine dimensionless discharge, Q_D from Fig. 3 where B/S refers to the homogeneous pre-mining magnitude.

In this work, the width ratio (W/t) varies from 20 to 200 and $\gamma H/E_m$ varies from $10^{-1.1}$ to $10^{-4.6}$. These ranges are chosen to include most practical applications.

VERIFICATION OF THE FEM MODEL

The validity of the proposed model may be best illustrated by direct comparison with field measurements taken around a working longwall panel. Two separate case studies are documented in the following. The first one is located in the Pittsburgh seam in southwestern Pennsylvania, U.S.A. This study is used to corroborate the development of the dewatering zone with the zone defined by a dramatic change of vertical conductivity K_y within the model. The second case study serves to verify measured dimensionless discharge rate into a mined panel against that predicted from the model.

Case study 1[20]

The use of this study serves to verify the impact of hydraulic conductivity change on development of a dewatering zone above the mined panel. The study site is located in Greene County in southwestern Pennsylvania. The terrain in this portion of the unglaciated Appalachian Plateau consists of rounded hills separated by narrow stream valleys with a topographic relief of 91.44 m (300 ft)–137.16 m (450 ft). The mine overburden consists of shale, mudstone, claystone, fire clay, sandstone, limestone and coal to thicknesses of between 198.12 m (650 ft) and 335.28 m (1100 ft) above the Pittsburgh coalbed.

Mining impact on hydrology. Water supplies overlying, or in near proximity to, the room and pillar mined area have had no reported negative impacts related to this type of mining. This situation appears to be in response to the relatively thick mine overburden of 149.35 m (490 ft) or more, between water supplies and the mine.

Analysis of the water supplies developed in the subsided strata overlying the longwall panels indicated 8 of 11 domestic water supplies that were monitored both before and after mining, were partly to completely dewatered. The maximum amount of dewatering appears to have been more extensive near longwall panel centers, and limited to the strata located at least 198.12 m (650 ft)–213.36 m (700 ft) above the base of the Pittsburgh coal. An examination of the ratio of panel width to mine overburden thickness indicated that dewatering at the mine occurred over a range of W/H ratio values of 0.75 to 1. This range of values corresponded to a minimum mine overburden thickness of 198.12 m (650 ft).

Water supplies located adjacent to but not above longwall panels were also examined for dewatering trends. Analysis of these supplies determined that dewatering zones were present, as defined by an angle of influence as illustrated in Fig. 4.

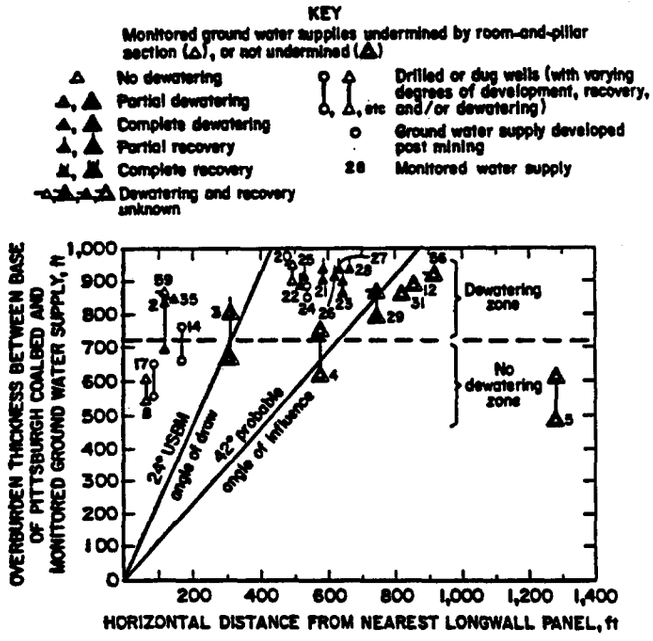

Fig. 4. Extent of dewatering of water supplies [21].

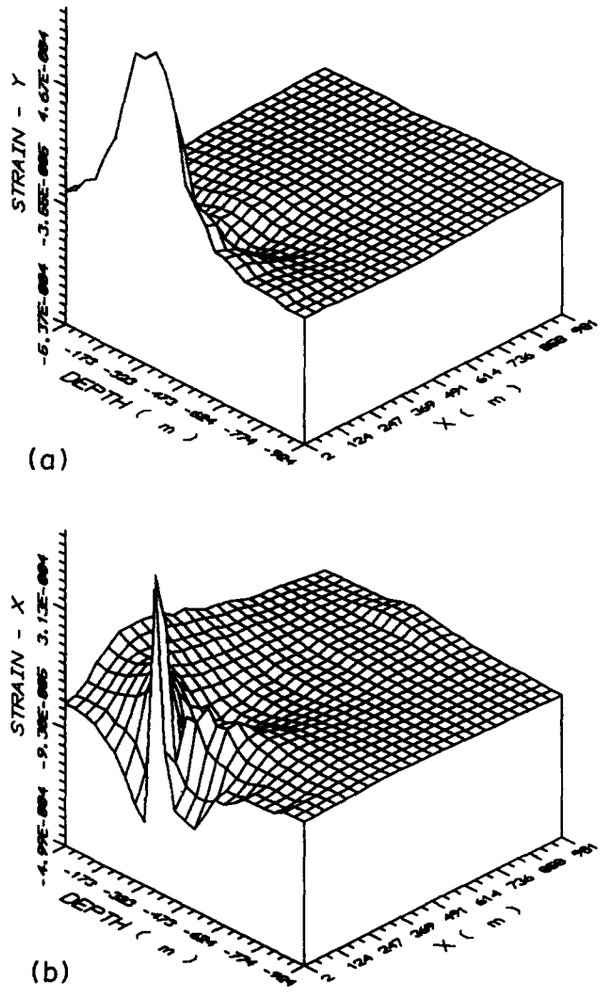

Fig. 5. Strain distributions (Case I).

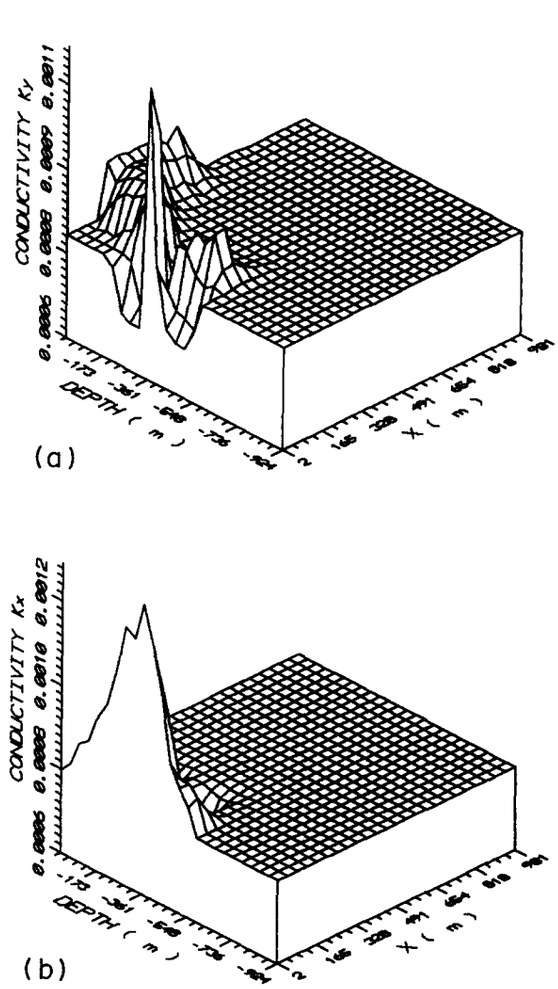

Fig. 6. Hydraulic conductivity distributions (Case I).

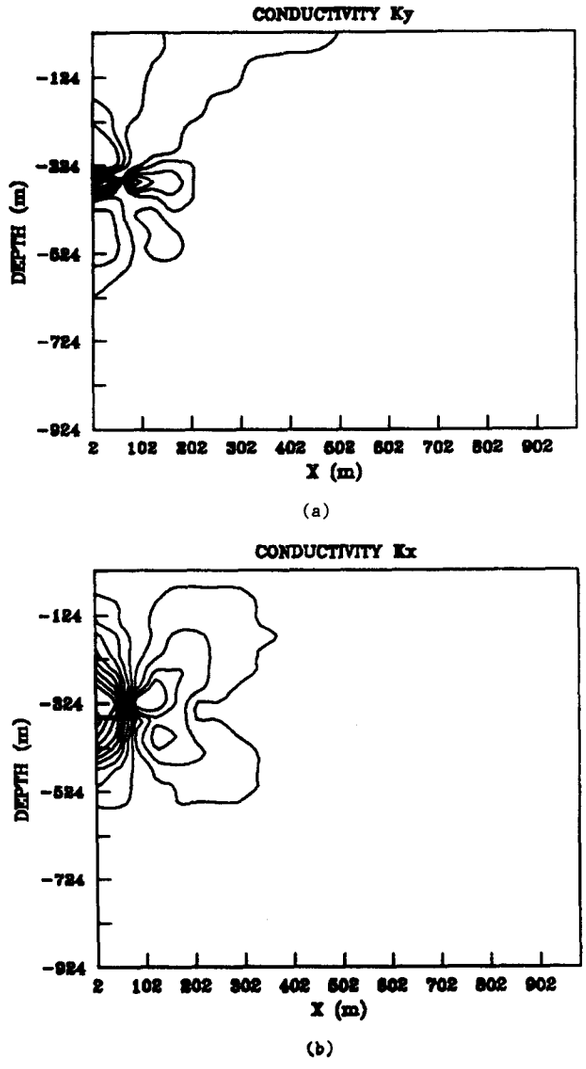

Fig. 7. Contour of hydraulic conductivities (Case I).

Numerical results. To demonstrate the influence of mining on conductivities, an initial fracture aperture B of 0.001 m and fracture spacing S of 1.0 m is used. This corresponds to a fracture porosity of 0.001. Other typical parameters for the overburden are: elastic modulus = 2.0×10^{10} Pa; Poisson's ratio = 0.25; and specific weight of overburden = 2700 kg/m^3. Calculated post-mining strains and hydraulic conductivity distributions in the vertical and horizontal directions are illustrated in Figs 5–7. The influence of the excavation is concentrated around the mined panel, as apparent in these figures.

By inspection, Fig. 7 illustrates that the angle of influence that defines the area of large conductivity change is approx. 40°. This is in agreement with the monitored results (influence angle of 42°) illustrated in Fig. 4. In this case study, calculated maximum horizontal strain occurs 250 m from the center of the panel, as shown in Fig. 8. Note also the maximum change in vertical conductivity at the surface coincides with the maximum value of horizontal strain. The panel width is 180 m. Correspondingly, the angle of draw is approx. 26° which closely approximates that of 24° estimated at the site.

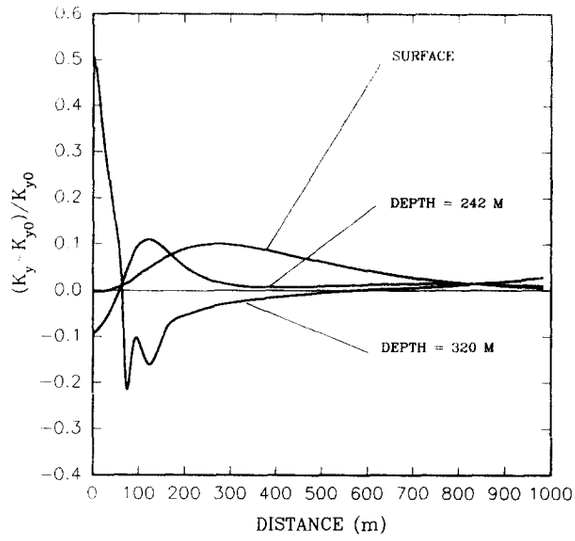

Fig. 8. Relative changes of hydraulic conductivity vs distance.

Case study II [21]

The Wistow mine in the U.K. works the Barnsley seam at depths between 271.27 m (890 ft) and 548.64 m (1800 ft). The average depth of the 2.44 m (8 ft–3.35 m) (11 ft) seam in the main is 365.76 m (1200 ft). The Permian strata overlying the Barnsley Coal Measure strata comprise Bunter sandstones, Lower Magnesian limestones and Basal sandstones. Calculated inflow rates within the thin beds are 2.21×10^{-2} m^3/sec (350 gpm). Flowrates in the strata immediately above the coal measure strata are high, being comparable with those of the Permian Bunter and Magnesium limestone.

The face was started at a depth of 360 m on 2nd July 1983. Probably because of the small thickness between the extracted Barnsley seam and the base of Permian strata, problems of frequent water inflow had been recorded. A water inflow averaging about 1.0102×10^{-1} m^3/sec (1600 gpm) occurred after a roof weighting. The face was 136 m (445 ft) long, extracting 2.44 m (8 ft) in a 3.28 m (10 ft) seam section. Fracture porosity B/S is assumed to be 3.0×10^{-4}. Typical rock parameters are as follows: Poisson's ratio $\nu = 0.25$, specific weight $\gamma = 2700$ kg/m^3, modulus of rock mass $E_m = 20$ GPa, fracture spacing $S = 1$ m.

From information available, the ratio of panel width to seam thickness W/t is 55.7 and the "equivalent compliance" $\gamma H/E_m$ is $10^{-3.32}$. From Fig. 3, the dimensionless flowrate is defined as 6×10^{-4} which corresponds closely to the measured flux of $Q = 1.0102 \times 10^{-1}$ m^3/sec (1600 gpm) or a dimensionless discharge of 5.1×10^{-4}.

CONCLUSIONS

The proposed finite element model is a powerful tool that incorporates the effect of strata deformation in defining changes in the subsurface hydrological regime. This makes it possible to assess the potential change in groundwater conditions around a panel that may result from mining. The model has an automeshing function

that allows variables to be readily changed in the numerical calculation.

The non-dimensional flux charts developed in this work provide a useful tool for straightforward practical use, for example, determination of groundwater flow into an excavation. Modulus reduction ratio may be used to define the severity of dewatering or conductivity enhancement, directly, rather than use of elusive joint stiffness parameters.

In conclusion, correct evaluation of inflow rate into a mined panel with the appropriate estimation of rock mass properties using the theory proposed in this paper throws new light on the behavior of this complex geological system. Further verification with field measurements and observations will encourage more sophisticated models to be developed in an attempt to better fit the observed behavior.

Acknowledgement—This work has been supported, in part, by the National Science Foundation under Grant No. MSS-9209059. This support is gratefully acknowledged.

Accepted for publication 14 December 1992.

REFERENCES

1. Elsworth D. *et al.* Groundwater effects of short-longwall (impact of mining on groundwater movement). Quarterly Report to Pennsylvania Energy Development Authority (1990).
2. Hill J. G. and Princ D. R. The impact of deep mining on an overlying aquifer in western Pennsylvania. *Ground Wat. Monitor. Rev.* **3,** 138–143 (1983).
3. Coe C. J. and Stowe S. M. Evaluating the impact of longwall coal mining on the hydrologic balance. In *The Impact of Mining on Ground Water, Proc. NWWA Conf.*, Denver, CO, pp. 348–359 (1984).
4. Booth C. J. Strata-movement concepts and the hydrogeological impact of underground coal mining. *Ground Wat.* **24,** 507–515 (1986).
5. Tieman G. E. and Rauch H. W. Study of Dewatering Effects at an Underground Longwall Mine Site in the Pittsburgh Seam of the Northern Appalachian Coalfield. Inf. Circ. 9173, U.S. Bureau of Mines, pp. 72–89 (1987).
6. Serafim J. L. and Campo del A. Interstitial pressures on rock foundations of dams. *J. Soil Mech. Found. Div., Am. Soc. Civil Engrs*, Vol. 91, SM5, pp. 65–85 (1965).
7. Elsworth D. Thermal permeability enhancement of blocky rocks: one dimensional flows. *Int. J. Rock Mech. Min. Sci. & Geomech. Abstr.* **26,** 329–339 (1989).
8. Walsh J. B. and Brace W. F. Elasticity of rock: a review of some recent theoretical studies. *Rock Mech. Engng Geol.* **4,** (1966).
9. Hobbs N. B. Factors affecting the prediction of settlement of structures on rock: with particular reference to the Chalk and Triass. In *Settlement of Structures*, pp. 579–610. Pentech Press, London (1975).
10. Iwai K. Fundamental studies of fluid flow through a single fracture. Ph.D. Dissertation, University of California, Berkeley (1976).
11. Witherspoon P. A., Wang Y. S. Y. and Gale J. E. Validity of cubic law for fluid flow in a deformable fracture, *Wat. Resour. Res.* **16,** 1016–1024 (1980).
12. Peres-Rodrigues F. About LNEC experience on scale effects in the deformability of rocks. *Proc. First Int. Workshop on Scale Effects in Rock Masses*, Loen, Norway, pp. 155–164 (1990).
13. Bieniawski Z. T. Engineering classification of jointed rock masses. *Trans. S. Afr. Inst. Civ. Engrs* **15,** 335–344 (1973).
14. Laubscher D. H. and Taylor H. W. The importance of Geomechanics Classification of jointed rock masses in mining operations. *Exploration for Rock Engineering* (Edited Z. T. Bieniawski), Vol. 1, pp. 119–128. Balkema, Rotterdam (1976).
15. Ferguson G. A. Optimization of block caving with a complex environment. *Min. Mag.* **140,** 126–139 (1979).
16. Bieniawski Z. T. and Orr C. M. Rapid site appraisal for dam foundations by the Geomechanics Classification. *Proc. 12th Int. Congr. on Large Dams*, Mexico City, pp. 483–501 (1976).
17. Steffen O. K. H. Research and development needs in data collection for rock engineering. *Exploration for Rock Engineering* (Edited by Z. T. Bieniawski), Vol. 2, pp. 93–104. Balkema, Rotterdam (1976).
18. Bieniawski Z. T. Determination rock mass deformability: experience from case histories. *Int. J. Rock Mech. Min. Sci.* **15,** 237–248 (1978).
19. Serafim J. L. and Pereira J. P. Considerations of the Geomechanics Classification of Bieniawski. *Proc. Int. Symp. on Engng Geol. and Underground Constr.*, LNEC, Lisbon, Portugal (1983).
20. Tieman G. E. and Rauch H. W. Study of dewatering effects at an underground longwall mine site in the Pittsburgh seam of the Northern Appalachian coalfield, Bureau of Mines Information Circular, IC 9137, pp. 72–89 (1987).
21. Tieman G. E. and H. W. Rauch Study of dewatering effects at an underground longwall mine site in the Pittsburgh seam of the Northern Appalachian coalfield. *Proc. Bureau of Mines Technology Transfer Seminar*, Pittsburgh, PA (1986).